

Connecting Neutrino Masses and Dark Matter by High-dimensional Lepton Number Violation Operator

Chao-Qiang Geng^{1,2,3*}, Da Huang^{2†}, Lu-Hsing Tsai^{2‡} and Qing Wang^{4,5§}

¹*Chongqing University of Posts & Telecommunications, Chongqing, 400065, China*

²*Department of Physics, National Tsing Hua University, Hsinchu, 300 Taiwan*

³*Physics Division, National Center for Theoretical Sciences, Hsinchu, 300 Taiwan*

⁴*Department of Physics, Tsinghua University, Beijing 100084, China*

⁵*Collaborative Innovation Center of Quantum Matter, Beijing 100084, China*

(Dated: September 25, 2021)

Abstract

We propose a new model with the Majorana neutrino masses generated at two-loop level, in which the lepton number violation (LNV) processes, such as neutrinoless double beta decays, are mainly induced by the dimension-7 LNV effective operator $\mathcal{O}_7 = \bar{l}_R^c \gamma^\mu L_L (D_\mu \Phi) \Phi \Phi$. Note that it is necessary to impose an Z_2 symmetry in order that \mathcal{O}_7 dominates over the conventional dimension-5 Weinberg operator, which naturally results in a stable Z_2 -odd neutral particle to be the cold dark matter candidate. More interestingly, due to the non-trivial dependence of the charged lepton masses, the model predicts the neutrino mass matrix to be in the form of the normal hierarchy. We also focus on a specific parameter region of great phenomenological interests, such as electroweak precision tests, dark matter direct searches along with its relic abundance, and lepton flavor violation processes.

PACS numbers: 11.30.Fs, 13.15.+g, 14.60.Lm, 14.60.Pq, 95.30.Cq

* geng@phys.nthu.edu.tw

† dahuang@phys.nthu.edu.tw

‡ lhstai@phys.nthu.edu.tw

§ wangq@mail.tsinghua.edu.cn

I. INTRODUCTION

The presence of the tiny neutrino masses and mixings between different neutrino flavors have been established by many neutrino oscillation experiments [1–7], while more and more evidences are accumulated for the existence of dark matter (DM) over the last several decades, with the most precise measurement of its relic abundance by PLANCK [8, 9]. Both phenomena cannot be explained within the Standard Model (SM), thus providing us with two windows towards new physics beyond it. An interesting idea is to connect neutrinos and DM in a unified framework as many existing attempts in the literature (see *e.g.* Refs. [10–13]). We would like to push this connection further in the present paper.

In order to understand the mass hierarchy problem in the neutrino sector, there are many models in the literature to naturally generate small Majorana neutrino masses such as the traditional Seesaw [14–26] and radiative mass generation mechanisms [10–13, 27–29]. Most of them can be summarized as a specific realization of the conventional dimension-5 Weinberg operator. However, the generation of Majorana neutrino masses only requires the lepton number violation (LNV) by two units, and there exist many other equally legitimate LNV effective operators [30–38], which are composed of the SM fields but with higher scaling dimensions. From the effective field theory perspective, it is generically believed that these high-dimensional effective operators are subdominated by the Weinberg operator due to the suppression from the corresponding high powers of the large cutoff. In order for these operators to show up as the leading contributions, one usually needs to impose an additional symmetry on the model to break the usual scaling arguments. Furthermore, if this symmetry is kept unbroken, then the lightest symmetry-protected neutral particle would provide a perfect DM candidate. In this way, the symmetry connects Majorana neutrino masses and DM physics by the high-dimensional effective operators. Such a connection has been already exemplified by some recent three-loop neutrino mass models [13, 39–41], which realize the dimension-9 effective operator $\mathcal{O}_9 = \bar{l}_R^c l_R [(D_\mu \Phi) \Phi]^2$ with the DM embedded in the loop.

In this study, we focus on a specific dimension-7 LNV operator $\mathcal{O}_7 = \bar{l}_R^c \gamma^\mu L_L (D_\mu \Phi) \Phi \Phi$ [32, 34, 37] and construct a UV complete model with an unbroken Z_2 symmetry to accomplish the above general arguments. In this model, Majorana neutrino masses arise radiatively at two-loop level, and neutrinoless double beta ($0\nu\beta\beta$) decays are dominated by a new “long-

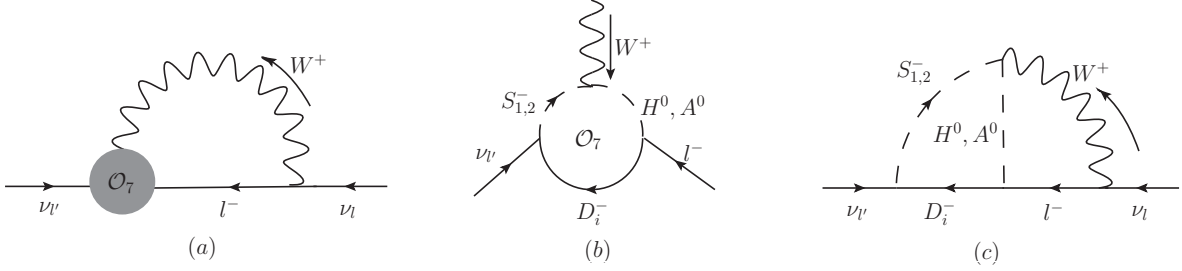


FIG. 1: Typical diagrams for (a) induced neutrino masses by the effective operator \mathcal{O}_7 , (b) the one-loop realization of \mathcal{O}_7 , and (c) the two-loop neutrino mass generation.

range” contribution¹, as the results of the existence of \mathcal{O}_7 , while DM can also be embedded naturally as the lightest Z_2 -odd neutral state.

This paper is organized as follows. In Sec. II, we first describe the particle content and write down the relevant part of the Lagrangian for the model. We then calculate the two-loop neutrino masses and new contributions to the $0\nu\beta\beta$ decay rate in the model, with the emphasis on their relations to the high-dimensional effective operator \mathcal{O}_7 . In Sec. III, the constraints on the model are addressed from the electroweak (EW) precision tests, dark matter searches, and lepton flavor violating (LFV) processes. Finally, we give the conclusions in Sec. IV.

II. GENERATION OF NEUTRINO MASSES AND $0\nu\beta\beta$ DECAYS

A. The Model

Fig. 1a shows the neutrino mass generation induced by the one-loop diagram with \mathcal{O}_7 . In order to produce \mathcal{O}_7 at one-loop level, we introduce two scalars: $s : (1, 2)$ and $\chi : (2, 1/2)$, and three vector-like fermions $D_{(L,R)i} : (2, 1/2)$ with $i = 1, 2$ and 3 to the SM under $SU(2)_L \times U(1)_Y$. A Z_2 symmetry is also imposed, in which only the new particles carry odd

¹ The definitions of “short” and “long” range contributions to $0\nu\beta\beta$ follow Refs. [42, 43].

charges. The relevant new parts of the Lagrangian are given by

$$\begin{aligned}
-\Delta L = & \mu_s^2(s^*s) + \mu_\chi^2(\chi^\dagger\chi) + V_4 + \left[\xi_{il} \overline{(D_{Li})^c} (i\sigma_2) L_{Li} s + \zeta_{il} \overline{(D_{Li})} l_{Ri} \chi + M_{Di} \bar{D}_{Li} D_{Ri} \right. \\
& \left. + \kappa s^* \chi^\dagger (i\sigma_2) \Phi + \frac{\lambda_5}{2} (\chi^\dagger \Phi)^2 + \text{H.c.} \right], \tag{1}
\end{aligned}$$

$$\begin{aligned}
V_4 = & \lambda_3 (\Phi^\dagger \Phi) (\chi^\dagger \chi) + \lambda_4 (\Phi^\dagger \chi) (\chi^\dagger \Phi) + \lambda_{\Phi s} (\Phi^\dagger \Phi) (s^* s) + \lambda_{\chi s} (\chi^\dagger \chi) (s^* s) \\
& + \lambda_\chi (\chi^\dagger \chi)^2 + \lambda_s (s^* s)^2, \tag{2}
\end{aligned}$$

where $\Phi = (\Phi^+, \Phi^0)^T$ is the SM Higgs doublet and σ_2 is the Pauli matrix for the $SU(2)_L$ gauge group. After the EW spontaneous symmetry breaking, Φ acquires a vacuum expectation value $v \equiv \sqrt{2} \langle \Phi^0 \rangle \simeq 246$ GeV, while $\mu_\chi^2 > 0$ is necessary for preserving the Z_2 symmetry. Notice that the lepton number is explicitly broken only when κ , λ_5 , and at least one of $\xi_{il} \zeta_{il}$ are non-zero simultaneously. For convenience, we define $M_s^2 = \mu_s^2 + \frac{1}{2} \lambda_{\Phi s} v^2$ and $M_\chi^2 = \mu_\chi^2 + \frac{1}{2} \lambda_\chi v^2$. The trilinear coupling constant κ in Eq. (1) makes s^\pm mix with χ^\pm , which can be formulated as

$$\begin{pmatrix} s^\pm \\ \chi^\pm \end{pmatrix} = \begin{pmatrix} c_\theta & -s_\theta \\ s_\theta & c_\theta \end{pmatrix} \begin{pmatrix} S_1^\pm \\ S_2^\pm \end{pmatrix}, \quad t_{2\theta} = \frac{\sqrt{2} \kappa v}{M_s^2 - M_\chi^2}, \tag{3}$$

where $s_x \equiv \sin x$, $c_x \equiv \cos x$, $t_x \equiv \tan x$, and S_1^\pm and S_2^\pm represent the charged mass eigenstates with their masses, given by

$$\begin{aligned}
M_{S_1}^2 &= \frac{c_\theta^2}{c_{2\theta}} M_s^2 - \frac{s_\theta^2}{c_{2\theta}} M_\chi^2, \\
M_{S_2}^2 &= \frac{c_\theta^2}{c_{2\theta}} M_\chi^2 - \frac{s_\theta^2}{c_{2\theta}} M_s^2, \tag{4}
\end{aligned}$$

respectively. On the other hand, λ_5 contributes to the mass splitting between H^0 and A^0 in χ , shown as

$$M_H^2 = M_\chi^2 + \frac{1}{2} (\lambda_4 + \lambda_5) v^2, \quad M_A^2 = M_\chi^2 + \frac{1}{2} (\lambda_4 - \lambda_5) v^2. \tag{5}$$

As for the new fermions, we have the tree-level relation $M_{D_i^\pm} = M_{D_i^0}$ for each D_i doublet. The mass splittings between the charge and neutral components of the inert fermion doublets can only be induced by loop corrections with values around a few hundred MeV [44].

In this paper, we will characterize the model by using the physical quantities:

$$M_H, M_A, M_{S_1}, M_{S_2}, M_{D_i}, s_\theta, \lambda_L, \xi_{il}, \text{ and } \zeta_{il}, \tag{6}$$

where $\lambda_L \equiv \frac{1}{2}(\lambda_3 + \lambda_4 + \lambda_5)$, and the other independent coupling constants from quarter terms:

$$\lambda_{\Phi_s}, \lambda_{\chi_s}, \lambda_\chi, \text{ and } \lambda_s, \quad (7)$$

which are less relevant in our discussion.

B. Two-Loop Majorana Neutrino Masses

As seen in Fig. 1b, the effective operator \mathcal{O}_7 can be induced by the one-loop diagram, whereas the Weinberg operator cannot². Consequently, Majorana neutrino masses appear through the two-loop diagram in Fig. 1c³. The resulting neutrino mass matrix M_ν defined in the Lagrangian $-\frac{1}{2}\overline{(\nu_L^c)}_l(M_\nu)_{ll'}(\nu_L)_{l'} + \text{H.c.}$ can be calculated as

$$(M_\nu)_{ll'} = -\frac{1}{(16\pi^2)^2} \frac{G_{FS2\theta}}{\sqrt{2}} (M_H^2 - M_A^2) \sum_{i=1,2,3} (m_l \zeta_{il} \xi_{il'} + m_{l'} \zeta_{i'l'} \xi_{il}) [I_{i1} - I_{i2}], \quad (8)$$

where m_l ($l = e, \mu, \tau$) are charged lepton masses, and I_{ij} are defined by

$$I_{ij} \equiv \int_0^1 dy_2 \int_0^{1-y_2} dy_1 \int_0^1 dx_3 \int_0^{1-x_3} dx_2 \int_0^{1-x_2-x_3} dx_1 \left\{ \left[\frac{2(1-3x)}{x(1-x)} + \frac{6y_1(2-x)}{(1-x)^2} \right] \log(m_{ij}^2) + \frac{-2y_1(2-x)}{x(1-x)} \frac{M_W^2}{m_{ij}^2} \right\}, \quad (9)$$

$$m_{ij}^2 \equiv y_1 [x_1 M_H^2 + x_2 M_A^2 + x_3 M_W^2] + y_2 x (1-x) M_{S_j}^2 + (1-y_1-y_2)x(1-x) M_{D_i}^2, \quad (10)$$

$$x = x_1 + x_2.$$

Subsequently, one can diagonalize M_ν by

$$\text{diag}(m_1, m_2, m_3) = V^T M_\nu V, \quad (11)$$

where $m_{1,2,3}$ are three neutrino mass eigenvalues, which can have the normal ordering, $m_1 < m_2 \ll m_3$, or inverted ordering, $m_3 \ll m_1 < m_2$, and V is the Pontecorvo-Maki-Nakagawa-Sakata mixing matrix [47, 48]. Without loss of generality, V can be written as the standard

² There is a similar realization of \mathcal{O}_7 in Ref. [37], in which a triplet replaced the singlet s of our model. A fundamental distinction of their paper from the present one is that \mathcal{O}_7 does not give the dominant contribution to Majorana neutrino masses in Ref. [37].

³ Similar topology with one W^\pm exchange in a two-loop neutrino mass model can also be found in Refs. [45, 46], in which a different high-dimensional effective operator is realized without DM.

parametrization by appropriate rephasing in L_L 's and l_R 's, given by [49]

$$V = \begin{pmatrix} c_{12}c_{13} & s_{12}c_{13} & s_{13}e^{-i\delta} \\ -s_{12}c_{23} - c_{12}s_{23}s_{13}e^{i\delta} & c_{12}c_{23} - s_{12}s_{23}s_{13}e^{i\delta} & s_{23}c_{13} \\ s_{12}s_{23} - c_{12}c_{23}s_{13}e^{i\delta} & -c_{12}s_{23} - s_{12}c_{23}s_{13}e^{i\delta} & c_{23}c_{13} \end{pmatrix} \begin{pmatrix} 1 & 0 & 0 \\ 0 & e^{i\alpha_{21}/2} & 0 \\ 0 & 0 & e^{i\alpha_{31}/2} \end{pmatrix}, \quad (12)$$

where the mixing angles with $s_{ij} \equiv \sin \theta_{ij}$ and $c_{ij} \equiv \cos \theta_{ij}$ are defined within $[0, \pi/2]$, and Dirac phase δ and Majorana phases α_{21} and α_{31} are defined within $[0, 2\pi]$.

From Eq. (8), we can get two important features for this mass generation mechanism. Firstly, the overall size of M_ν is proportional to the mass difference of the neutral scalars, $M_H^2 - M_A^2$, and the combined factor of the charged states, $s_{2\theta}(I_{i1} - I_{i2})$, in which the former is generated by λ_5 and the latter corresponds to the size of κ . Turning off one of them will make all neutrinos massless. Secondly, the neutrino masses are positively correlated to the coupling matrix elements ξ_{il} and ζ_{il} , as well as the sizes of m_l . As the existence of the charged lepton mass hierarchy, $m_e \ll m_\mu < m_\tau$, if both matrices of (ξ_{il}) and (ζ_{il}) are in uniform textures, the magnitude of $(M_\nu)_{ee}$ should be much smaller than those of other M_ν entries. We make a great advantage of this general expectation by taking the following limit

$$(M_\nu)_{ee} \simeq 0, \quad (13)$$

which is shown in Refs. [49, 50] to rule out the inverted ordering of neutrino mass spectrum at more than 2σ confident level. Thus, the normal ordering is predicted for the present model. Note that in the limit of Eq. (13), Ref. [49] even shows that the lightest neutrino mass m_1 can only be located within the range $0.001\text{eV} \lesssim m_1 \lesssim 0.01\text{eV}$. Moreover, the smallness of $(M_\nu)_{ee}$ is also required by the $0\nu\beta\beta$ decay, which will be clear in the next subsection.

If we further focus on the CP conserving case, *i.e.*, $\delta, \alpha_{21}, \alpha_{31} = 0$ or π , then m_1 will be constrained in the two narrow regimes, around 0.002 and 0.007 eV with $\{\delta, \alpha_{21}, \alpha_{31}\} = \{0, \pi, 0\}$ (Texture A) or $\{\pi, \pi, 0\}$ (Texture B) and $\{0, \pi, \pi\}$ (Texture C) or $\{\pi, \pi, \pi\}$ (Texture D), respectively. Taking the central values of $\theta_{12}, \theta_{23}, \theta_{13}, \Delta m_{21}^2$, and Δm_{32}^2 from the global fitting for the neutrino oscillation data [49], the corresponding mass matrices for Textures A, B, C, and D (T_A, T_B, T_C and T_D) are given by

$$T_A : M_\nu = \begin{pmatrix} 0 & 0.12 & 0.92 \\ 0.12 & 1.9 & 2.7 \\ 0.92 & 2.7 & 2.4 \end{pmatrix} (10^{-2}) \text{eV}, \quad (14)$$

$$\text{T}_B : M_\nu = \begin{pmatrix} 0 & -0.90 & -0.24 \\ -0.90 & 1.7 & 2.7 \\ -0.24 & 2.7 & 2.6 \end{pmatrix} (10^{-2}) \text{ eV}, \quad (15)$$

$$\text{T}_C : M_\nu = \begin{pmatrix} 0 & -1.1 & -0.055 \\ -1.1 & -2.3 & -2.1 \\ -0.055 & -2.1 & -3.1 \end{pmatrix} (10^{-2}) \text{ eV}, \quad (16)$$

$$\text{T}_D : M_\nu = \begin{pmatrix} 0 & -0.086 & 1.1 \\ -0.086 & -2.6 & -2.2 \\ 1.1 & -2.2 & -2.9 \end{pmatrix} (10^{-2}) \text{ eV}, \quad (17)$$

respectively.

We now search for possible coupling matrix forms to realize the above four CP conserving neutrino textures. For simplicity, hereafter we will take $M_{D1} = M_{D2} = M_{D3} = M_D$, and also set ξ proportional to the identity matrix with the diagonal matrix element to be ξ_d . Taking a symmetric form of ζ , the mass matrix element should be proportional to $\xi_d \zeta_{\nu l} (m_l + m_\nu)$. We remark that by an appropriate phase absorption to the fermion fields, one can always have a positive ξ_d without loss of generality. Comparing with Eqs. (14)-(17), the forms of $\zeta_{ll'}$ in the four neutrino matrix textures can be obtained as

$$\begin{aligned} \text{T}_A : \zeta &\propto \begin{pmatrix} \times & 0.12 & 0.052 \\ 0.12 & 0.89 & 0.14 \\ 0.052 & 0.14 & 0.068 \end{pmatrix}, \quad \text{T}_B : \zeta \propto \begin{pmatrix} \times & -0.84 & -0.013 \\ -0.84 & 0.82 & 0.14 \\ -0.013 & 0.14 & 0.072 \end{pmatrix}, \\ \text{T}_C : \zeta &\propto \begin{pmatrix} \times & -1. & -0.0031 \\ -1. & -1.1 & -0.11 \\ -0.0031 & -0.11 & -0.088 \end{pmatrix}, \quad \text{T}_D : \zeta \propto \begin{pmatrix} \times & -0.081 & 0.062 \\ -0.081 & -1.2 & -0.12 \\ 0.062 & -0.12 & -0.081 \end{pmatrix}, \end{aligned} \quad (18)$$

where the cross means that the value of ζ_{ee} is still arbitrary at this stage, which will be constrained by $0\nu\beta\beta$ decays. The overall scale of $\zeta_{ll'}$ can be determined by Eq. (8) when all new particle masses, s_θ and ξ_d are known. We will also leave the discussion about the correlation between ξ and ζ from the LFV constraints to Sec. III.

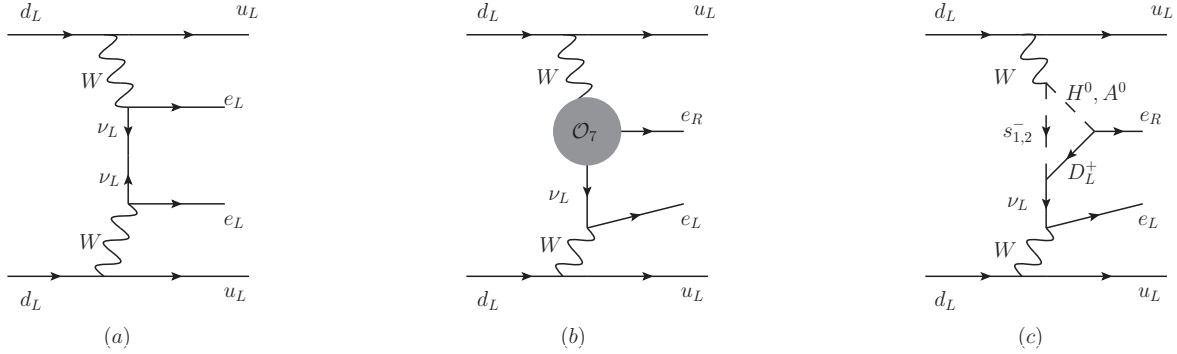


FIG. 2: Diagrams for $0\nu\beta\beta$ decays from (a) the traditional processes with the neutrino mass insertion on the propagator, (b) the contribution involving \mathcal{O}_7 , and (c) the one-loop construction which realizes \mathcal{O}_7 . For (b) and (c), the corresponding upside-down diagrams also need to be considered.

C. Neutrinoless Double Beta Decay

In the previous section, we have built a two-loop neutrino mass model in which the LNV operator \mathcal{O}_7 provides the leading contribution. The next step is to study the LNV effect in this model induced by this high-dimensional operator. The most sensitive smoking gun for the LNV is the $0\nu\beta\beta$ decay, which will place the strong constraint on $\xi_d\zeta_{ee}$ and $(M_\nu)_{ee}$.

For the Majorana neutrino masses, there always exists the traditional long-range decay process by the exchange of neutrinos with a pair of left-handed electrons emitted as shown in Fig. 2a. Note that there is a chirality flipping on the internal neutrino propagator, which leads to the proportionality of the amplitude to the neutrino mass matrix element $(M_\nu)_{ee}$, in the sense that the detection for $0\nu\beta\beta$ processes could help to determine or constrain $|(M_\nu)_{ee}|$. However, it is known that in some types of neutrino models, Fig. 2a does not give the main part of this process, and one should have *a priori* consideration on the effects of other new diagrams. For example, a class of neutrino models [51–53] that can be characterized by the dimension-9 operator $\mathcal{O}_9 = \bar{l}_R^c l_R [(D_\mu \Phi)^T (i\sigma_2) \Phi] [(D^\mu \Phi)^T (i\sigma_2) \Phi]$ is well studied in Refs. [51, 52, 54–56], and the new contribution is much larger than that from Fig. 2a by orders of magnitude of 10^8 . For our model or those with \mathcal{O}_7 as the main LNV source, the $0\nu\beta\beta$ decays are dominated by the diagram in Fig. 2b, which is not suppressed by the nearly-vanishing $(M_\nu)_{ee}$. We can write down a general formula for the half lifetime $T_{1/2}^{0\nu\beta\beta}$ of

the $0\nu\beta\beta$ decay with the contributions from Figs. 2a and 2b, given by [57]

$$[T_{1/2}^{0\nu\beta\beta}]^{-1} = C_{mm} \left(\frac{M_{ee}}{m_e} \right)^2 + C_{\eta\eta} \eta^2 + C_{m\eta} \left(\frac{M_{ee}}{m_e} \right) \eta, \quad (19)$$

$$\eta = -\frac{1}{16\pi^2} \frac{s_{2\theta} \xi \zeta_{ee}}{4} (M_H^2 - M_A^2) (I'_1 - I'_2), \quad (20)$$

with

$$I'_j = \int_0^1 dx_3 \int_0^{1-x_3} dx_2 \int_0^{1-x_2-x_3} dx_1 \frac{1}{x_1 M_H^2 + x_2 M_A^2 + x_3 M_{S_j}^2 + (1-x_1-x_2-x_3) M_D^2},$$

where C_{mm} , $C_{m\eta}$, and $C_{\eta\eta}$ include the phase space integrations and nuclear matrix elements defined in Ref. [57], and η is the coupling of the interaction $(4G_F/\sqrt{2})(\bar{u}_L\gamma_\mu d_L)(\bar{l}_R\gamma^\mu\nu_L^c)$, which is originated from the one-loop generation for \mathcal{O}_7 (in Fig. 2c). By using the numerical results therein and also in Ref. [58], we find that the contribution proportional to $C_{\eta\eta}$ is much larger than those to C_{mm} and $C_{m\eta}$.

As given in Eq. (20) that η is proportional to $\xi_d \zeta_{ee}$, the upper bound on $|\xi_d \zeta_{ee}|$ can be obtained by comparing with the current experimental sensitivities on $T_{1/2}^{0\nu\beta\beta}$ [59–65] in Table I, where we have used $M_H = 70\text{GeV}$, $M_A = 95\text{GeV}$, $M_{S_1} = 310\text{GeV}$, $M_{S_2} = 90\text{GeV}$, $M_D = 200\text{GeV}$, and $s_\theta = 0.1$. The strongest constraint is $|\xi_d \zeta_{ee}| < 2.8 \times 10^{-4}$, given by the target nucleus Xe. Finally, the contribution from \mathcal{O}_7 (proportional to $C_{\eta\eta}$) is much larger than that from $(M_\nu)_{ee}$ (proportional to C_{mm}) by a factor of $\mathcal{O}(10^{-4})$, because the latter is greatly suppressed by the factor of m_e/v . On the other hand, lifting up $|(M_\nu)_{ee}|$ to the average size of $M_\nu \sim 10^{-2}\text{eV}$ will result in the excess of the $0\nu\beta\beta$ decay rates that conflict with the observations. Table I also shows the maximum value of $(M_\nu)_{ee}$ for each nucleus.

TABLE I: Constraints on $|\xi_d \zeta_{ee}|$ from $0\nu\beta\beta$ for different nuclei as the targets. The corresponding limitation on $|M_\nu|_{ee}$ are also given.

	$> T_{\text{exp}}(10^{25}\text{yr})$	$C_{\eta\eta}(10^{25}\text{yr})^{-1}$	$ \xi_d \zeta_{ee} _{\text{max}}$	$ M_\nu _{ee}(10^{-2})\text{eV}$
GERDA-1(^{76}Ge) [59]	2.1	4.4×10^{-9}	3.6×10^{-4}	< 0.017
KamLAND-Zen(^{136}Xe) [60]	1.9	8.3×10^{-9}	2.8×10^{-4}	< 0.013
NEMO-3(^{150}Nd) [62]	0.0018	2.9×10^{-7}	1.5×10^{-3}	< 0.072
CUORICINO(^{130}Te) [63]	0.3	2.3×10^{-8}	4.2×10^{-4}	< 0.02
NEMO-3(^{82}Se) [64, 65]	0.036	1.5×10^{-8}	1.5×10^{-3}	< 0.07
NEMO-3(^{100}Mo) [65]	0.11	3.5×10^{-8}	5.6×10^{-4}	< 0.027

Finally, we end this section by mentioning that the role of the Z_2 symmetry is to make the dimension-7 operator \mathcal{O}_7 become the dominant contributions to in the LNV processes and Majorana neutrino masses. Note that as the quantum numbers of the doublet (χ) and the singlet (s) scalars are the same as those in the Zee's model [27], the Majorana neutrino masses would be mainly generated by the corresponding one-loop diagrams related to the conventional Weinberg operator if the Z_2 symmetry is absent. However, with the Z_2 symmetry, \mathcal{O}_7 is singled out at 1-loop level, while other LNV effective operators, especially the dimension-5 Weinberg operator, are much suppressed since they would be only induced by higher-loop diagrams. In this way, the Z_2 symmetry breaks the conventional effective operator ordering based on the scaling dimensions. Other LNV effects, like $0\nu\beta\beta$ decays, would also change the leading modes accordingly.

III. PHENOMENOLOGICAL CONSTRAINTS

A. Electroweak Precision Tests

As discussed previously, in order to have the two-loop neutrino masses in our model, the non-zero coupling constants λ_5 and κ are both required. The former splits the masses between H^0 and A^0 , and the latter mixes the charged states χ^\pm and s^\pm which carry different EW gauge quantum numbers. Both effects could change the values of the EW oblique S and T parameters. In particular, the T parameter should yield a stronger constraint on this model. The deviation of T from the SM is given by [13]

$$\Delta T = \frac{1}{4\pi s_W^2 M_W^2} \left[\frac{s_\theta^2}{4} (F_{S_1^\pm, H^0} + F_{S_1^\pm, A^0}) + \frac{c_\theta^2}{4} (F_{S_2^\pm, H^0} + F_{S_2^\pm, A^0}) - \frac{1}{2} c_\theta^2 s_\theta^2 F_{S_1^\pm, S_2^\pm} - \frac{1}{4} F_{H^0, A^0} \right], \quad (21)$$

with the function F defined by

$$F_{x,y} = \frac{M_x^2 + M_y^2}{2} - \frac{M_x^2 M_y^2}{M_x^2 - M_y^2} \log \left(\frac{M_x^2}{M_y^2} \right). \quad (22)$$

The value of $F_{x,y}$ becomes zero when $M_x \rightarrow M_y$, and it increases with the mass splitting among the new scalars. Note that ΔT has little to do with D_i since there is neither mixing between D_i and the SM leptons nor tree-level mass splitting among D_i , while the deviation for the S parameter can also be ignored [66]. The formulae of Eq. (21) is a general result

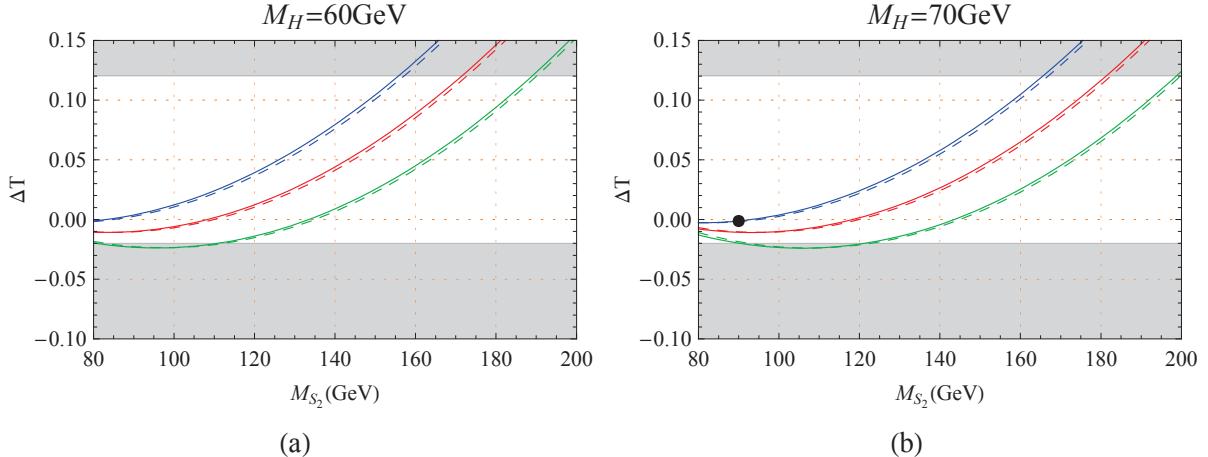


FIG. 3: Plots of ΔT versus M_{S_2} with (a) $M_H = 60$ GeV and (b) $M_H = 70$ GeV, where blue, red, and green colors represent $M_A - M_H = 25, 50,$ and 75 GeV, respectively, and solid (dashed) curve corresponds to $s_\theta = 0.1$ (0), while the black dot is the benchmark point discussed in Sec.III.D.

for the models with the mixings between the inert doublet and singlet scalars. The global fitting results constrain ΔT at $1.5 - 1.7\sigma$ deviation by $-0.02 < \Delta T < 0.12$ [49]. We show ΔT as a function of M_{S_2} in Fig. 3, where we have used $M_{S_1} = 310$ GeV and $s_\theta = 0.1(0)$ along with (a) $M_H = 60$ and (b) 70 GeV. It is obvious that the numerical result of our model with $s_\theta = 0.1$ is approximately equal to a pure inert doublet model with $s_\theta = 0$. In general, ΔT goes up with increasing M_{S_2} , and for a large value of $M_A - M_H$, the constraint on M_{S_2} becomes stronger. The figure also shows that $M_A - M_H$ is limited to be less than 75 GeV for $M_H = 60$ to 70 GeV and $90 \lesssim M_{S_2} \lesssim 110$ GeV. Finally, it should be noted that M_{S_2} can not be too small, since there exists a lower bound on M_{S_2} located within 70 to 90 GeV [67] from the LEP experiments.

B. Dark Matter

In this model, the lightest of the extra neutral particles: H^0 , A^0 , and $D_{1,2,3}^0$ could be a DM candidate, whose stability is guaranteed by the imposed Z_2 symmetry. In the following, we will focus on the case that DM is constituted solely by H^0 with a small charged scalar mixing s_θ , in which our DM would be very similar to that in the well-studied inert doublet model [68–70]. Furthermore, we concentrate on the low DM mass region with 50 GeV $\leq M_H \leq 80$ GeV [69, 70], in which a large H^0 - A^0 mass splitting can be allowed for the

generation of the right two-loop neutrino masses. In addition, the mass of S_2^\pm should be higher than 90 GeV in order to escape the LEP bounds [67], so that the co-annihilation channels, such as H^0-A^0 and $H^0-S_2^\pm$, would be strongly suppressed and thus ignored.

We use the package micrOMEGAs [71] to accurately calculate the relic abundance Ω_H in the above parameter space, including all possible annihilations and co-annihilations. When M_H approaches the half of the SM Higgs mass $M_h/2 \simeq 62.5$ GeV [72, 73], the Higgs resonance in the s -channel would become prominent, which is characterized by the coupling λ_L controlling the trilinear vertex $(\lambda_L v)hH^0H^0$. However, in other regions, the DM annihilation cross section is dominated by the $WW^{(*)}$ mode. Therefore, the correct DM relic abundance is achieved mainly by the balance of the $WW^{(*)}$ and Higgs resonance channels. Fig. 4 shows the relevant parameter space in the $M_H-|\lambda_L|$ plane, which can give the observed DM abundance $0.112 \lesssim \Omega_H h^2 \lesssim 0.128$ at 3σ level [8, 9, 49]. Note that when DM is heavier than 73 GeV, the $WW^{(*)}$ channel would give a too large annihilation cross section to accommodate the DM relic abundance [69, 70], which is omitted in Fig. 4.

The DM H^0 in this low mass region could be constrained by the DM direct detection experiments. Since we need a relatively large Higgs-mediation annihilation channel to generate DM relic abundance, the Higgs exchange channel can also give rise to sizeable spin-independent signals, with the corresponding DM-nucleon cross section as follows [69]:

$$\sigma_{H^0 N} = \frac{m_r^2}{4\pi} \left(\frac{\lambda_L}{M_H M_h^2} \right)^2 f^2 m_N^2. \quad (23)$$

Currently, the most stringent bound on the spin-independent DM-nucleon cross section is provided by the LUX experiment [74], with the minimum cross section of 7.6×10^{-46} cm² for a DM mass of 33 GeV. It is shown in Fig. 4 that the LUX experiment has already probed some parameter space required by the DM relic abundance. Especially, the low DM mass region with $M_H \leq 52$ GeV is actually ruled out, as indicated by the shaded area in the plot. However, most parameter spaces are still allowed by LUX.

C. Lepton Flavor Violation

The current experimental constraints on LFV processes, such as the radiative decays $l \rightarrow l'\gamma$ [75, 76], $\mu - e$ conversions [77–80], and three-lepton decays $l \rightarrow l_1 l_2 \bar{l}_3$ [81, 82], are all dominated by one-loop diagrams with Z_2 odd particles inside. We take $\mu \rightarrow e\gamma$ as an

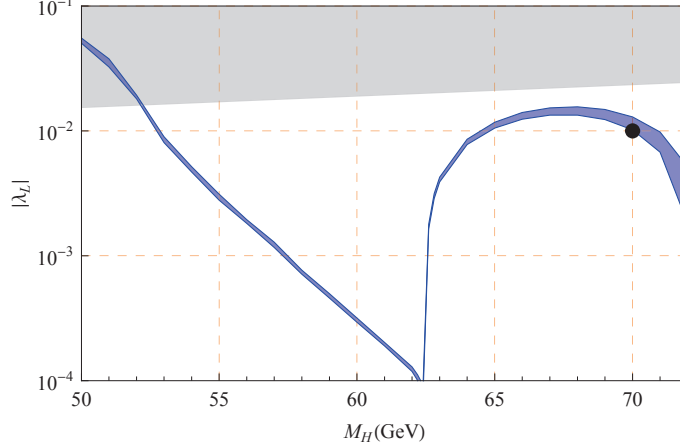


FIG. 4: The parameter space for the correction DM relic abundance in the $M_H - |\lambda_L|$ plane, with the blue band representing the region within 3σ deviation of the cold dark matter relic abundance. The gray shaded area is excluded by the LUX experiment, and the black dot represents the benchmark point. This plot is calculated with $M_A = 95$ GeV and $M_{S_2} = 90$ GeV.

illustration because the current experimental upper bound $\text{Br}(\mu^+ \rightarrow e^+ \gamma) < 5.7 \times 10^{-13}$ [75] usually constrains a model in the most stringent way. In our model, we have

$$\begin{aligned} \text{Br}(\mu^\mp \rightarrow e^\mp \gamma) &= \frac{\Gamma(\mu^\mp \rightarrow e^\mp \gamma)}{\Gamma(\mu^\mp \rightarrow e^\mp \nu \bar{\nu})} \\ &= \frac{3\alpha_e}{64\pi G_F^2} \left| \sum_l \zeta_{l\mu} \zeta_{le} \right|^2 \left(s_\theta^2 K_{S_1} + c_\theta^2 K_{S_2} + \frac{1}{2} K'_H + \frac{1}{2} K'_A \right)^2, \end{aligned} \quad (24)$$

where the loop integrals K_x and K'_x are defined as

$$K_x = \frac{2z^3 + 3z^2 - 6z + 1 - 6z^2 \log z}{6(1-z)^4 M_x^2}, \quad K'_x = -\frac{z^3 - 6z^2 + 3z + 2 + 6z \log z}{6(1-z)^4 M_x^2}, \quad (25)$$

with $z = M_D^2/M_x^2$. As is expected, the decay branching ratio is proportional to the coupling constant combination $\left| \sum_l \zeta_{l\mu} \zeta_{le} \right|^2$. On the other hand, when the values of $\xi_d \zeta_{lW}$ are fixed by the neutrino masses, the only degree of freedom left is the size of ξ_d . When ξ_d is large, ζ_{lW} should be suppressed, along with all the relevant LFV processes. This feature can be displayed in Fig. 5, where ζ_{lW} are expressed in the forms given in Eq. (18), with the unknown ζ_{ee} satisfying the relation $|\xi_d \zeta_{ee}| \lesssim 10^{-4}$, as well as $s_\theta = 0.1$, $M_H = 70$, $M_A = 95$, $M_{S_1} = 310$, $M_{S_2} = 90$ and 120 and $M_D = 200$ GeV. We find that the texture $T_{C(D)}$ yields the most stringent (weakest) constraint on ξ_d , such that $\xi_d \gtrsim 0.01$ (0.002) is required for $M_{S_2} = 90$ GeV. From another angle, if we set $\xi_d = 0.005$ with T_A , we can predict that

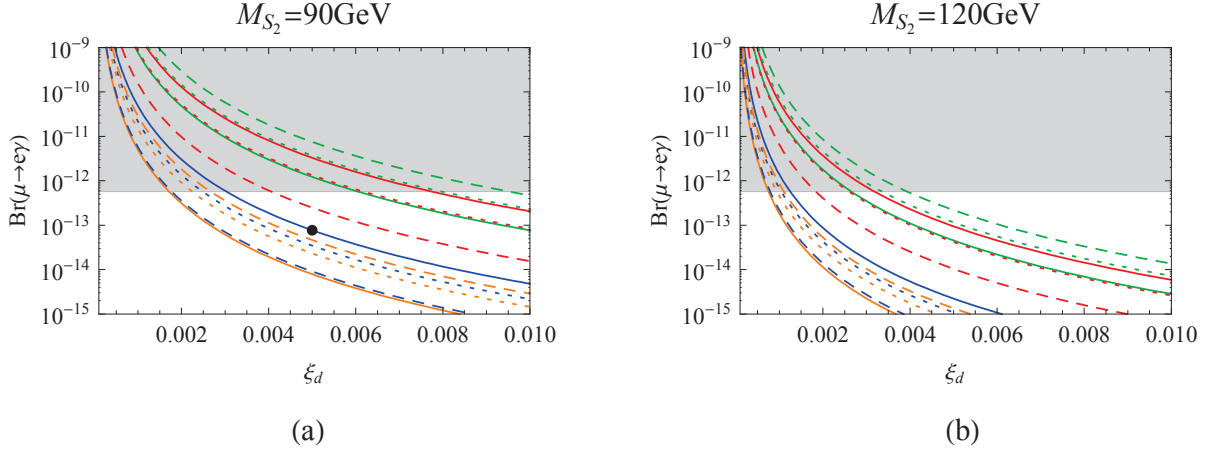


FIG. 5: $\text{Br}(\mu \rightarrow e\gamma)$ versus ξ , with (a) $M_{S_2} = 90 \text{ GeV}$ and (b) $M_{S_2} = 120 \text{ GeV}$, where the blue, red, green, and yellow curves correspond to the neutrino textures T_A , T_B , T_C , and T_D , respectively, while the black dot is the benchmark point.

$\text{Br}(\mu \rightarrow e\gamma) = 10^{-13}$ (3×10^{-15}) for $M_{S_2} = 90$ (120) GeV, which might be measured by the next-generation experiments in the future.

D. Numerical Results

Based on the above constraints from the LFV processes, EW precision tests, direct searches of DM with the required relic abundance, we find a benchmark point from the allowed parameter space, given by:

$$\begin{aligned}
 M_H = 70 \text{ GeV} , M_A = 95 \text{ GeV} , M_{S_1} = 310 \text{ GeV} , M_{S_2} = 90 \text{ GeV} , \\
 M_{D_1} = M_{D_2} = M_{D_3} = M_D = 200 \text{ GeV} , s_\theta = 0.1 , \lambda_L = 0.01 ,
 \end{aligned} \tag{26}$$

and

$$\xi = \begin{pmatrix} 0.005 & 0. & 0. \\ 0. & 0.005 & 0. \\ 0. & 0. & 0.005 \end{pmatrix} , \quad \zeta = \begin{pmatrix} 0.02 & 0.005 & 0.0022 \\ 0.005 & 0.038 & 0.0061 \\ 0.0022 & 0.0061 & 0.0029 \end{pmatrix} . \tag{27}$$

It is clear that the matrix ζ corresponds to the neutrino texture T_A . We also plot this benchmark point by a black dot in Figs. 5a, 3b, and 4, where the experimental results

from LFV processes, oblique parameters, and DM searches are well satisfied, respectively. Finally, from the benchmark point, one can obtain $\lambda_3 = 0.155$, $\lambda_4 = -0.067$, $\lambda_5 = -0.068$, $\kappa = 50.3 \text{ GeV}$, $\mu_\chi = 65.5 \text{ GeV}$, and $M_S = 309 \text{ GeV}$, which are all small enough to ensure the self-consistence of the perturbation theory.

IV. CONCLUSIONS

We have tried to make the connection between neutrino physics and dark matter searches. In particular, we have emphasized that every effective operator, which violates the lepton number by two units, can give an equally good mechanism to generate Majorana neutrino masses. The problem lies in the fact that the new high-dimensional operators might be buried by the overwhelming effects from the conventional Weinberg operator which possess the smallest scaling dimension. One way to break this effective field theory ordering is to impose some symmetry which would protect the lightest neutral symmetry-protected states to be the DM particle.

We have explicitly realized this connection by constructing a UV complete model with the Z_2 symmetry to generate the dimension-7 operator $\mathcal{O}_7 = \bar{l}_R^c \gamma^\mu L_L (D_\mu \Phi) \Phi \Phi$. We have shown that the Majorana neutrino mass matrix structure and the leading $0\nu\beta\beta$ decay contribution are closely related to \mathcal{O}_7 . Especially, the neutrino mass matrix is predicted to be of the normal ordering due to the hierarchy in the charged lepton masses, and the $0\nu\beta\beta$ decay rate can be large enough to be tested in the next-generation experiments. If we impose an additional CP symmetry in the lepton sector, we can even determine the form of the neutrino mass matrix completely. We have also focused on a specific parameter region with a small mixing between charged scalars, and considered the constraints from the electroweak precision tests, dark matter searches, and LFV processes.

Acknowledgments

This work was supported by National Center for Theoretical Sciences, National Science Council (Grant No. NSC-101-2112-M-007-006-MY3) and National Tsing Hua University (Grant No. 104N2724E1), the National Science Foundation of China (NSFC Grant No. 11475092), the Tsinghua University Initiative Scientific Research Program (Grant No.

20121088494).

-
- [1] P. Anselmann *et al.* [GALLEX Collaboration], Phys. Lett. B **285**, 390 (1992).
 - [2] Y. Fukuda *et al.* [Super-Kamiokande Collaboration], Phys. Rev. Lett. **81**, 1562 (1998) [hep-ex/9807003].
 - [3] Q. R. Ahmad *et al.* [SNO Collaboration], Phys. Rev. Lett. **89**, 011301 (2002) [nucl-ex/0204008].
 - [4] Q. R. Ahmad *et al.* [SNO Collaboration], Phys. Rev. Lett. **89**, 011302 (2002) [nucl-ex/0204009].
 - [5] M. H. Ahn *et al.* [K2K Collaboration], Phys. Rev. D **74**, 072003 (2006) [hep-ex/0606032].
 - [6] K. Abe *et al.* [T2K Collaboration], Phys. Rev. Lett. **107**, 041801 (2011) [arXiv:1106.2822 [hep-ex]].
 - [7] F. P. An *et al.* [Daya Bay Collaboration], Phys. Rev. Lett. **108**, 171803 (2012) [arXiv:1203.1669 [hep-ex]].
 - [8] P. A. R. Ade *et al.* [Planck Collaboration], Astron. Astrophys. **571**, A16 (2014) [arXiv:1303.5076 [astro-ph.CO]].
 - [9] R. Adam *et al.* [Planck Collaboration], arXiv:1502.01582 [astro-ph.CO].
 - [10] L. M. Krauss, S. Nasri and M. Trodden, Phys. Rev. D **67**, 085002 (2003) [hep-ph/0210389].
 - [11] E. Ma, Phys. Rev. D **73**, 077301 (2006) [hep-ph/0601225].
 - [12] M. Aoki, S. Kanemura and O. Seto, Phys. Rev. Lett. **102**, 051805 (2009) [arXiv:0807.0361 [hep-ph]].
 - [13] M. Gustafsson, J. M. No and M. A. Rivera, Phys. Rev. Lett. **110**, no. 21, 211802 (2013) [Erratum-ibid. **112**, no. 25, 259902 (2014)] [arXiv:1212.4806 [hep-ph]].
 - [14] P. Minkowski, Phys. Lett. B **67**, 421 (1977).
 - [15] T. Yanagida, in *Proceedings of the Workshop on the Unified Theory and the Baryon Number in the Universe*, edited by O. Sawada and A. Sugamoto (KEK, Tsukuba, 1979), p. 95.
 - [16] M. Gell-Mann, P. Ramond, and R. Slansky, in *Supergravity*, edited by P. van Nieuwenhuizen and D. Freedman (North-Holland, Amsterdam, 1979), p. 315.
 - [17] S. L. Glashow, in *Proceedings of the 1979 Cargese Summer Institute on Quarks and Leptons*, edited by M. Levy *et al.* (Plenum Press, New York, 1980), p. 687.

- [18] R. N. Mohapatra and G. Senjanovic, Phys. Rev. Lett. **44**, 912 (1980).
- [19] M. Magg and C. Wetterich, Phys. Lett. B **94**, 61 (1980).
- [20] J. Schechter and J. W. F. Valle, Phys. Rev. D **22**, 2227 (1980).
- [21] T. P. Cheng and L. F. Li, Phys. Rev. D **22**, 2860 (1980).
- [22] G. B. Gelmini and M. Roncadelli, Phys. Lett. B **99**, 411 (1981).
- [23] G. Lazarides, Q. Shafi and C. Wetterich, Nucl. Phys. B **181**, 287 (1981).
- [24] R. N. Mohapatra and G. Senjanovic, Phys. Rev. D **23**, 165 (1981).
- [25] J. Schechter and J. W. F. Valle, Phys. Rev. D **25**, 774 (1982).
- [26] R. Foot, H. Lew, X. G. He and G. C. Joshi, Z. Phys. C **44**, 441 (1989).
- [27] A. Zee, Phys. Lett. B **93**, 389 (1980) [Erratum-ibid. B **95**, 461 (1980)].
- [28] A. Zee, Nucl. Phys. B **264**, 99 (1986).
- [29] K. S. Babu, Phys. Lett. B **203**, 132 (1988).
- [30] K. S. Babu and C. N. Leung, Nucl. Phys. B **619**, 667 (2001) [hep-ph/0106054].
- [31] A. de Gouvea and J. Jenkins, Phys. Rev. D **77**, 013008 (2008) [arXiv:0708.1344 [hep-ph]].
- [32] F. del Aguila, A. Aparici, S. Bhattacharya, A. Santamaria and J. Wudka, JHEP **1206**, 146 (2012) [arXiv:1204.5986 [hep-ph]].
- [33] P. W. Angel, N. L. Rodd and R. R. Volkas, Phys. Rev. D **87**, no. 7, 073007 (2013) [arXiv:1212.6111 [hep-ph]].
- [34] F. del guila, A. Aparici, S. Bhattacharya, A. Santamaria and J. Wudka, PoS Corfu **2012**, 028 (2013) [arXiv:1305.4900 [hep-ph]].
- [35] P. W. Angel, Y. Cai, N. L. Rodd, M. A. Schmidt and R. R. Volkas, JHEP **1310**, 118 (2013) [JHEP **1411**, 092 (2014)] [arXiv:1308.0463 [hep-ph]].
- [36] Y. Cai, J. D. Clarke, M. A. Schmidt and R. R. Volkas, JHEP **1502**, 161 (2015) [arXiv:1410.0689 [hep-ph]].
- [37] A. Aparici, arXiv:1312.0554 [hep-ph].
- [38] J. C. Helo, M. Hirsch, T. Ota and F. A. P. d. Santos, arXiv:1502.05188 [hep-ph].
- [39] C. Q. Geng, D. Huang and L. H. Tsai, Phys. Rev. D **90**, no. 11, 113005 (2014) [arXiv:1410.7606 [hep-ph]].
- [40] L. G. Jin, R. Tang and F. Zhang, Phys. Lett. B **741**, 163 (2015) [arXiv:1501.02020 [hep-ph]].
- [41] C. Q. Geng, D. Huang and L. H. Tsai, Phys. Lett. B **745**, 56 (2015) [arXiv:1504.05468 [hep-ph]].

- [42] F. F. Deppisch, M. Hirsch and H. Pas, *J. Phys. G* **39**, 124007 (2012) [arXiv:1208.0727 [hep-ph]].
- [43] F. Bonnet, M. Hirsch, T. Ota and W. Winter, *JHEP* **1303**, 055 (2013) [*JHEP* **1404**, 090 (2014)] [arXiv:1212.3045 [hep-ph]].
- [44] M. Cirelli and A. Strumia, *New J. Phys.* **11**, 105005 (2009) [arXiv:0903.3381 [hep-ph]].
- [45] K. S. Babu and J. Julio, *Nucl. Phys. B* **841**, 130 (2010) [arXiv:1006.1092 [hep-ph]].
- [46] K. S. Babu and J. Julio, *Phys. Rev. D* **85**, 073005 (2012) [arXiv:1112.5452 [hep-ph]].
- [47] B. Pontecorvo, *Sov. Phys. JETP* **6**, 429 (1957) [*Zh. Eksp. Teor. Fiz.* **33**, 549 (1957)].
- [48] Z. Maki, M. Nakagawa and S. Sakata, *Prog. Theor. Phys.* **28**, 870 (1962).
- [49] K. A. Olive *et al.* [Particle Data Group Collaboration], *Chin. Phys. C* **38**, 090001 (2014).
- [50] S. Pascoli, S. T. Petcov and L. Wolfenstein, *Phys. Lett. B* **524**, 319 (2002) [hep-ph/0110287].
- [51] C. S. Chen, C. Q. Geng and J. N. Ng, *Phys. Rev. D* **75**, 053004 (2007) [hep-ph/0610118].
- [52] C. S. Chen, C. Q. Geng, J. N. Ng and J. M. S. Wu, *JHEP* **0708**, 022 (2007) [arXiv:0706.1964 [hep-ph]].
- [53] C. Q. Geng and L. H. Tsai, arXiv:1503.06987 [hep-ph].
- [54] F. del Aguila, A. Aparici, S. Bhattacharya, A. Santamaria and J. Wudka, *JHEP* **1205**, 133 (2012) [arXiv:1111.6960 [hep-ph]].
- [55] M. Gustafsson, J. M. No and M. A. Rivera, *Phys. Rev. D* **90**, 013012 (2014) [arXiv:1402.0515 [hep-ph]].
- [56] S. F. King, A. Merle and L. Panizzi, *JHEP* **1411**, 124 (2014) [arXiv:1406.4137 [hep-ph]].
- [57] K. Muto, E. Bender and H. V. Klapdor, *Z. Phys. A* **334**, 187 (1989).
- [58] M. Doi, T. Kotani and E. Takasugi, *Prog. Theor. Phys. Suppl.* **83**, 1 (1985).
- [59] M. Agostini *et al.* [GERDA Collaboration], *Phys. Rev. Lett.* **111**, no. 12, 122503 (2013) [arXiv:1307.4720 [nucl-ex]].
- [60] A. Gando *et al.* [KamLAND-Zen Collaboration], *Phys. Rev. C* **85**, 045504 (2012) [arXiv:1201.4664 [hep-ex]].
- [61] A. Gando *et al.* [KamLAND-Zen Collaboration], *Phys. Rev. Lett.* **110**, no. 6, 062502 (2013) [arXiv:1211.3863 [hep-ex]].
- [62] J. Argyriades *et al.* [NEMO Collaboration], *Phys. Rev. C* **80**, 032501 (2009) [arXiv:0810.0248 [hep-ex]].
- [63] C. Arnaboldi *et al.* [CUORICINO Collaboration], *Phys. Rev. C* **78**, 035502 (2008)

- [arXiv:0802.3439 [hep-ex]].
- [64] R. Arnold *et al.* [NEMO Collaboration], Phys. Rev. Lett. **95**, 182302 (2005) [hep-ex/0507083].
- [65] A. S. Barabash *et al.* [NEMO Collaboration], Phys. Atom. Nucl. **74**, 312 (2011) [arXiv:1002.2862 [nucl-ex]].
- [66] F. del Aguila, J. de Blas and M. Perez-Victoria, Phys. Rev. D **78**, 013010 (2008) [arXiv:0803.4008 [hep-ph]].
- [67] A. Pierce and J. Thaler, JHEP **0708**, 026 (2007) [hep-ph/0703056 [HEP-PH]].
- [68] R. Barbieri, L. J. Hall and V. S. Rychkov, Phys. Rev. D **74**, 015007 (2006) [hep-ph/0603188].
- [69] L. Lopez Honorez and C. E. Yaguna, JHEP **1009**, 046 (2010) [arXiv:1003.3125 [hep-ph]].
- [70] For a recent study and further references, see *e.g.* A. Arhrib, Y. L. S. Tsai, Q. Yuan and T. C. Yuan, JCAP **1406**, 030 (2014) [arXiv:1310.0358 [hep-ph]].
- [71] G. Belanger, F. Boudjema and A. Pukhov, arXiv:1402.0787 [hep-ph].
- [72] G. Aad *et al.* [ATLAS Collaboration], Phys. Lett. B **716**, 1 (2012) [arXiv:1207.7214 [hep-ex]].
- [73] S. Chatrchyan *et al.* [CMS Collaboration], Phys. Lett. B **716**, 30 (2012) [arXiv:1207.7235 [hep-ex]].
- [74] D. S. Akerib *et al.* [LUX Collaboration], Phys. Rev. Lett. **112**, 091303 (2014) [arXiv:1310.8214 [astro-ph.CO]].
- [75] J. Adam *et al.* [MEG Collaboration], Phys. Rev. Lett. **110**, 201801 (2013) [arXiv:1303.0754 [hep-ex]].
- [76] B. Aubert *et al.* [BaBar Collaboration], Phys. Rev. Lett. **104**, 021802 (2010) [arXiv:0908.2381 [hep-ex]].
- [77] W. H. Bertl *et al.* [SINDRUM II Collaboration], Eur. Phys. J. C **47**, 337 (2006).
- [78] A. Badertscher, K. Borer, G. Czapek, A. Fluckiger, H. Hanni, B. Hahn, E. Hugentobler and H. Kaspar *et al.*, Lett. Nuovo Cim. **28**, 401 (1980).
- [79] C. Dohmen *et al.* [SINDRUM II. Collaboration], Phys. Lett. B **317**, 631 (1993).
- [80] W. Honecker *et al.* [SINDRUM II Collaboration], Phys. Rev. Lett. **76**, 200 (1996).
- [81] U. Bellgardt *et al.* [SINDRUM Collaboration], Nucl. Phys. B **299**, 1 (1988).
- [82] K. Hayasaka, K. Inami, Y. Miyazaki, K. Arinstein, V. Aulchenko, T. Aushev, A. M. Bakich and A. Bay *et al.*, Phys. Lett. B **687**, 139 (2010) [arXiv:1001.3221 [hep-ex]].